Supporting Information

Understanding microscopic binding mechanism of hydroxylated and sulfated polybrominated diphenyl ethers with transthyretin by molecular docking, molecular dynamics simulations and binding free energy calculations

Huiming Cao, Yuzhen Sun, Ling Wang, Chunyan Zhao, Jianjie Fu and Aiqian Zhang*

Molecular docking methods

AutoDock. Docking simulations of lamarkian genetic algorithm were performed by AutoDock 4.2.6[1] with 100 GA runs of each ligand. The active pocket of ligands binding was determined with a T4-centered grid box of 60 × 60 × 60 Å. The remaining parameters were set to default values to insure consistency during the entire calculations.

AutoDock Vina. Necessary PDBQT files for the receptor and ligand were prepared by using AutodockTools 1.5.4. Docking scores were calculated by the default scoring function[2].

idock. Similar to the docking method of AutoDock Vina[2], idock adopt a modification scoring function to predict binding affinity, and an optimization algorithm to explore the conformational space[3]. Necessary PDBQT files of docking calculations abided by the preparations of AutoDock Vina[2]. RF score[4] was used to rank the binding affinity of ligands.

iGEMdock. The standard docking settings (population size 200, 70 generations, and 3 numbers of solutions) were used to search the ligand-protein interactions based on genetic algorithm. iGEMdock scoring function[5] was chosen to evaluate the hydrophobic and electrostatic contributions to ligand preference.

CDocker. The parameters of CHARMm force field were assigned for receptor structure. The ligand conformations are generated using high-temperature molecular dynamics with different random seeds. The pose with the highest -CDOCKER interaction energy[6] was chosen to rank the binding affinity of ligands.

Libdock. The binding site was defined as a sphere space including all residues within 8 Å from native ligand T4. Other docking parameters were set to default values by DS software.

Surflex-Dock. The fragment growing algorithm[7] was used to search binding pose of ligands in TTR. Sybyl X1.2 software package was employed to prepare the binding site and subsequent docking calculations. Total score (TS) expressed in negative logarithm of dissociation constant (Kd) was used to rank the binding affinity of ligands.

LeDock. All parameters were set to default for conformation sampling by a combination of simulated annealing and evolutionary optimization. Binging pocket and docking parameters were prepared by LePro module of LeDock programs (www.lephar.com).

Table S1 Experimental binding potencies of the target compounds.

compound	RBA	logRBA
2'-OH-BDE-03	0.15[a],0.06[b]	-0.96
2'-OH-BDE-07	0.3[a],0.3[b]	-0.52
2'-OH-BDE-28	3[a],0.29[b]	0.22
2'-OH-BDE-68	3.75[a]	0.57
3-OH-BDE-154	3[a],1.3[b]	0.33
3-OH-BDE-47	4.29[a],2.36[b],4[c]	0.55
3'-OH-BDE-07	0.6[a],0.69[b]	-0.19
3'-OH-BDE-28	1[a],0.72[b]	-0.07
4-OH-BDE-42	3.33[a],3.5[c],0.9[f]	0.41
4'-OH-BDE-17	1.5[a]	0.18
4'-OH-BDE-49	3[a],3.5[c]	0.51
5-OH-BDE-47	7.5[a],1.19[b],3[c]	0.59
6-OH-BDE-47	2[a],0.8[b],0.39[c],0.31[d],0.41[f]	-0.11
6-OH-BDE-85	4.29[a]	0.63
3-OH-BDE-100	1.19[b]	0.08
4-OH-BDE-188	1.37[b]	0.14
2'-OH-BDE-66	0.65[c],1.13[f]	-0.05
4'-OH-BDE-30	0.41[e]	-0.39
4'-OH-BDE-69	1.22[e]	0.09
4'-OH-BDE-121	1.42[e]	0.15

RBA:relative binding affinity; log RBA: logarithm of relative binding affinity.

[a] Experimental RBA for TTR-binding assay cited from Cao et al.[8]

[b] Experimental RBA for TTR-binding assay cited from Ren et al.[9]

[c] Experimental RBA for TTR-binding assay cited from Hamers et al.[10]

[d] Experimental RBA for TTR-binding assay cited from Hamers et al.[11]

[e] Experimental RBA for TTR-binding assay cited from Meerts et al.[12]

[f] Experimental RBA for TTR-binding assay cited from Montaño et al.[13]

Table S2 LeDock scores for the Cdk2 Kinase Inhibitors extracted from the ref 14.

Compound	IC_{50} (uM)	log IC_{50}	LeDock score
34	0.97	-0.013	-8.29
35	0.0054	-2.267	-10.04
36	5	0.698	-7.32
37	2.8	0.447	-7.45
38	1.2	0.079	-7.75
39	2.8	0.447	-8.06
40	2.3	0.361	-8.48
41	0.4	-0.397	-8.94
42	1.8	0.255	-8.56
43	1.7	0.23	-8.77
44	0.069	-1.161	-8.7
45	0.65	-0.187	-8.48
46	0.007	-2.154	-10.11
47	0.056	-1.251	-9.58
48	0.063	-1.2	-9.36
49	0.1	-1	-9.69
50	0.07	-1.154	-9.86
51	0.21	-0.677	-9.43
52	0.2	-0.698	-9.4
53	0.2	-0.698	-9.42
54	0.3	-0.522	-9.35
55	0.8	-0.096	-8.41
56	0.13	-0.886	-9.78
57	0.3	-0.522	-9.02

Table S3 The distance between O atom of –OH group of T4 and O atom of –OH group of Ser117 sidechain in the TTR-T4 crystal structures.

TTR-T4		$d_{O\text{-}O}$(Å)	
PDB id	species	Chain A	Chain B
1ETA	Homo sapiens	4.8	5.6
1ETB	Homo sapiens	5.6	5.6
1ICT	Homo sapiens	4.2	3.7
1SN0	Sparus aurata	7.2	7.0
2ROX	Homo sapiens	5.7	5.4

Table S4 Mean values of Rg for apo TTR and 6 TTR-ligand complexes during 30 ns MD simulations.

	apo	2'-OH-BDE-28	2'-Sulf-BDE-28	3-OH-BDE-47	3-Sulf-BDE-47	4-OH-BDE-47	4-Sulf-BDE-42
Rg	22.150	22.147	22.143	22.139	22.093	22.093	22.119

Table S5 RESP charges of B3LYP/cc-pVTZ and HF/6-31G* for the 2'-OH-BDE-28 and 2'-Sulf-BDE-28 simulation systems.

	2'-OH-BDE-28	2'-OH-BDE-28			2'-Sulf-BDE-28	2'-Sulf-BDE-28	
Atom name	B3LYP/cc-pVTZ	HF/6-31G*	D-value	Atom name	B3LYP/cc-pVTZ	HF/6-31G*	D-value
C1	-0.11	-0.17	0.06	C1	0.02	-0.06	0.08
C2	-0.19	-0.20	0.01	C2	-0.17	-0.17	0.00
C3	0.04	0.03	0.01	C3	-0.06	-0.08	0.02
C4	-0.37	-0.37	0.00	C4	-0.34	-0.33	-0.01
C5	0.49	0.48	0.01	C5	0.40	0.38	0.03
C6	0.09	0.18	-0.09	C6	0.05	0.17	-0.13
O1	-0.52	-0.57	0.05	O1	-0.45	-0.50	0.05
C7	0.85	0.90	-0.05	C7	0.64	0.69	-0.04
C8	-0.50	-0.54	0.04	C8	-0.36	-0.39	0.03
C9	0.17	0.19	-0.02	C9	0.10	0.09	0.01
C10	-0.37	-0.41	0.04	C10	-0.31	-0.32	0.01
C11	0.42	0.43	-0.02	C11	0.35	0.35	0.01
C12	-0.58	-0.62	0.04	C12	-0.46	-0.48	0.02
Br1	-0.04	-0.04	0.00	Br1	-0.09	-0.09	-0.01
Br2	0.01	0.01	0.00	Br2	-0.06	-0.05	-0.01
O2	-0.52	-0.61	0.10	O2	-0.29	-0.41	0.12
Br3	-0.05	-0.04	0.00	Br3	-0.12	-0.11	-0.02
H1	0.13	0.16	-0.03	H1	0.12	0.16	-0.04
H2	0.11	0.13	-0.02	H2	0.11	0.13	-0.02
H3	0.19	0.21	-0.02	H3	0.18	0.20	-0.02
H4	0.20	0.23	-0.03	H4	0.18	0.22	-0.04
H5	0.10	0.12	-0.02	H5	0.12	0.14	-0.02
H6	0.03	0.05	-0.02	H6	0.02	0.04	-0.02
H7	0.42	0.47	-0.04	S1	1.04	1.26	-0.22
				O3	-0.54	-0.62	0.07
				O4	-0.54	-0.62	0.07
				O5	-0.54	-0.62	0.07

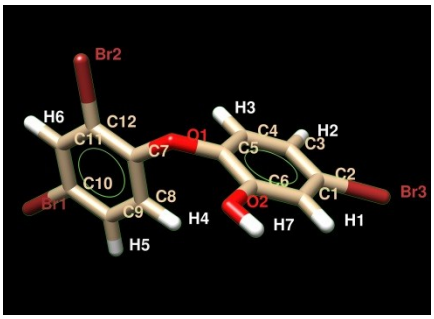

2'-OH-BDE-28

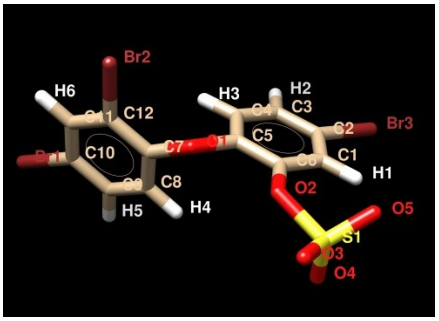

2'-Sulf-BDE-28

Table S6 RESP charges of B3LYP/cc-pVTZ and HF/6-31G* for the 3-OH-BDE-47 and 3-Sulf-BDE-47 simulation systems.

	3-OH-BDE-47	3-OH-BDE-47			3-Sulf-BDE-47	3-Sulf-BDE-47	
Atom name	B3LYP/cc-pVTZ	HF/6-31G*	D-value	Atom name	B3LYP/cc-pVTZ	HF/6-31G*	D-value
C1	0.82	0.96	-0.14	C1	0.90	1.03	-0.13
C2	-0.46	-0.55	0.09	C2	-0.51	-0.61	0.10
C3	0.19	0.24	-0.06	C3	0.21	0.26	-0.05
C4	-0.54	-0.61	0.07	C4	-0.54	-0.59	0.05
C5	0.91	1.00	-0.09	C5	0.88	0.95	-0.07
C6	-0.79	-0.88	0.09	C6	-0.75	-0.82	0.08
O1	-0.59	-0.65	0.06	O1	-0.59	-0.65	0.06
C7	0.88	0.93	-0.05	C7	0.86	0.91	-0.05
C8	-0.48	-0.52	0.04	C8	-0.48	-0.51	0.02
C9	0.16	0.18	-0.02	C9	0.13	0.14	-0.01
C10	-0.35	-0.39	0.04	C10	-0.34	-0.37	0.03
C11	0.42	0.43	-0.02	C11	0.40	0.41	0.00
C12	-0.65	-0.69	0.04	C12	-0.63	-0.66	0.03
Br1	-0.03	-0.03	0.00	Br1	-0.08	-0.07	-0.01
Br2	0.03	0.03	0.00	Br2	-0.01	0.00	-0.01
Br3	0.00	0.01	-0.01	Br3	-0.04	-0.02	-0.02
Br4	0.04	0.04	0.00	Br4	0.04	0.05	-0.01
O2	-0.55	-0.65	0.10	O2	-0.47	-0.56	0.10
H1	0.10	0.12	-0.02	H1	0.06	0.08	-0.02
H2	0.20	0.22	-0.02	H2	0.17	0.20	-0.02
H3	0.20	0.22	-0.02	H3	0.19	0.21	-0.02
H4	0.10	0.12	-0.02	H4	0.10	0.12	-0.02
H5	0.04	0.06	-0.02	H5	0.04	0.06	-0.02
H6	0.38	0.43	-0.05	S1	1.00	1.22	-0.23
				O3	-0.51	-0.59	0.07
				O4	-0.51	-0.59	0.07
				O5	-0.51	-0.59	0.07

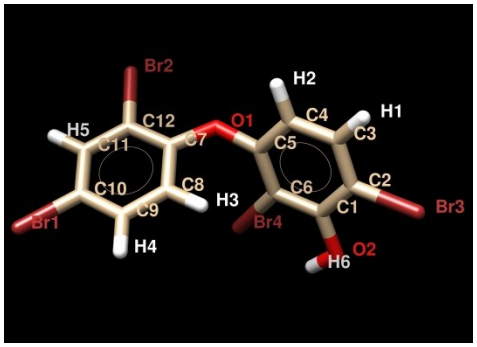

3-OH-BDE-47

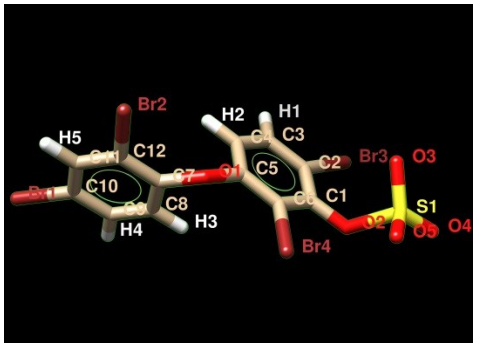

3-Sulf-BDE-47

Table S7 RESP charges of B3LYP/cc-pVTZ and HF/6-31G* for the 4-OH-BDE-42 and 4-Sulf-BDE-42 simulation systems.

	4-OH-BDE-42	4-OH-BDE-42			4-Sulf-BDE-42	4-Sulf-BDE-42	
Atom name	B3LYP/cc-pVTZ	HF/6-31G*	D-value	Atom name	B3LYP/cc-pVTZ	HF/6-31G*	D-value
C1	-0.04	-0.11	0.07	C1	-0.05	-0.10	0.05
C2	0.38	0.50	-0.12	C2	0.36	0.47	-0.11
C3	-0.33	-0.40	0.06	C3	-0.18	-0.25	0.07
C4	-0.20	-0.19	-0.01	C4	-0.33	-0.30	-0.03
C5	0.58	0.60	-0.02	C5	0.60	0.62	-0.02
C6	-0.31	-0.30	-0.01	C6	-0.30	-0.31	0.00
O1	-0.56	-0.62	0.06	O1	-0.58	-0.63	0.06
C7	0.83	0.90	-0.06	C7	0.89	0.95	-0.06
C8	-0.45	-0.49	0.04	C8	-0.49	-0.52	0.03
C9	0.14	0.16	-0.02	C9	0.13	0.15	-0.02
C10	-0.35	-0.38	0.04	C10	-0.34	-0.38	0.04
C11	0.40	0.42	-0.02	C11	0.44	0.46	-0.01
C12	-0.62	-0.67	0.05	C12	-0.69	-0.73	0.04
Br1	-0.04	-0.03	0.00	Br1	-0.09	-0.07	-0.01
Br2	0.02	0.02	0.00	Br2	0.04	0.04	0.00
O2	-0.55	-0.65	0.10	O2	-0.34	-0.45	0.11
Br3	0.02	0.02	0.00	Br3	-0.05	-0.04	-0.01
Br4	0.00	0.01	-0.01	Br4	-0.06	-0.05	-0.01
H1	0.17	0.19	-0.03	H1	0.15	0.18	-0.03
H2	0.16	0.18	-0.02	H2	0.17	0.19	-0.02
H3	0.19	0.21	-0.02	H3	0.19	0.21	-0.02
H4	0.10	0.12	-0.02	H4	0.10	0.12	-0.02
H5	0.04	0.06	-0.02	H5	0.02	0.04	-0.02
H6	0.42	0.47	-0.05	S1	1.04	1.25	-0.21
				O3	-0.54	-0.61	0.07
				O4	-0.54	-0.61	0.07
				O5	-0.54	-0.61	0.07

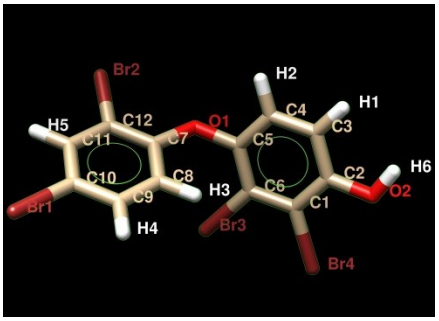

4-OH-BDE-42

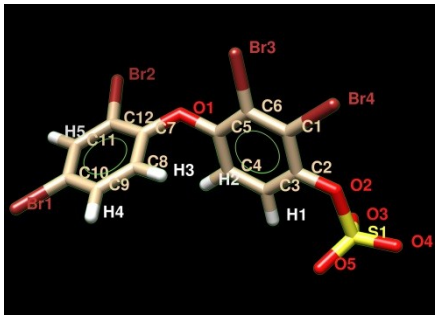

4-Sulf-BDE-42

Table S8 Ligand binding free energy components[a] of TTR-ligand complex simulation systems (Unit: kcal/mol; RESP charge: HF/6-31G*; GB^{OBC1} model: igb=2).

Compounds	ΔE_{vdw}	ΔG_{SA}	ΔE_{ele}	ΔG_{GB}	ΔG_{calc}
3-OH-BDE-47	-44.41 (2.00)	-4.37 (0.12)	-6.48 (2.09)	18.22(1.58)	-37.05 (2.11)
3-Sulf-BDE-47	-47.25 (3.03)	-5.33 (0.18)	98.38 (7.70)	-88.28 (6.43)	-42.49 (4.13)

[a] $\Delta G_{cal} = \Delta E_{vdw} + \Delta G_{SA} + \Delta E_{elc} + \Delta G_{GB}$. Standard error of mean values is displayed in parenthesis.

Table S9 Ligand binding free energy components of neutral and anionic forms for 3-OH-BDE-47 and 3-Sulf-BDE-47, respectively (Unit: kcal/mol; GB^{OBC1} model: igb=2).

Systems	Molecular form	ΔE_{vdw}	ΔG_{SA}	ΔE_{ele}	ΔG_{GB}	ΔG_{calc}
3-OH-BDE-47	Anionic form	-43.78 (2.33)	-4.40 (0.12)	101.15 (7.92)	-93.70 (7.31)	-40.74 (2.44)
3-Sulf -BDE-47	Neutral form	-48.00 (2.29)	-5.28 (0.16)	-6.76 (3.27)	17.29 (1.85)	-42.75 (2.84)

[a] $\Delta G_{cal} = \Delta E_{vdw} + \Delta G_{SA} + \Delta E_{elc} + \Delta G_{GB}$. Standard error of mean values is displayed in parenthesis.

Table S10 Computational alanine scanning results ($\Delta\Delta G_{cal}$) for the key interaction residues.

Systems	Lys15	Lys15'	Ser117	Ser117'
2'-OH-BDE-28	-0.52	-1.25	-0.15	-0.47
2'- Sulf-BDE-28	-5.03	-4.00	-0.11	-0.04
3-OH-BDE-47	-1.13	-0.65	-0.80	-0.14
3- Sulf-BDE-47	-1.78	-2.64	-0.54	-3.66
4-OH-BDE-42	-1.02	-0.88	-0.21	-3.96
4- Sulf-BDE-42	-3.86	-4.85	-0.16	-0.09

Table S11 Ligand binding free energy components of flipped poses (Unit: kcal/mol; GB^{OBC1} model: igb=2).

Compounds	ΔE_{vdw}	ΔG_{SA}	ΔE_{ele}	ΔG_{GB}	ΔG_{calc}
3-Sulf-BDE-47	-42.54 (3.62)	-4.87 (0.35)	81.49 (16.89)	-72.33(15.88)	-38.27 (3.55)
4-Sulf-BDE-42	-45.50 (2.29)	-5.42 (0.16)	114.96 (7.32)	-99.64 (5.73)	-35.60 (3.64)

[a] $\Delta G_{cal} = \Delta E_{vdw} + \Delta G_{SA} + \Delta E_{elc} + \Delta G_{GB}$. Standard error of mean values is displayed in parenthesis.

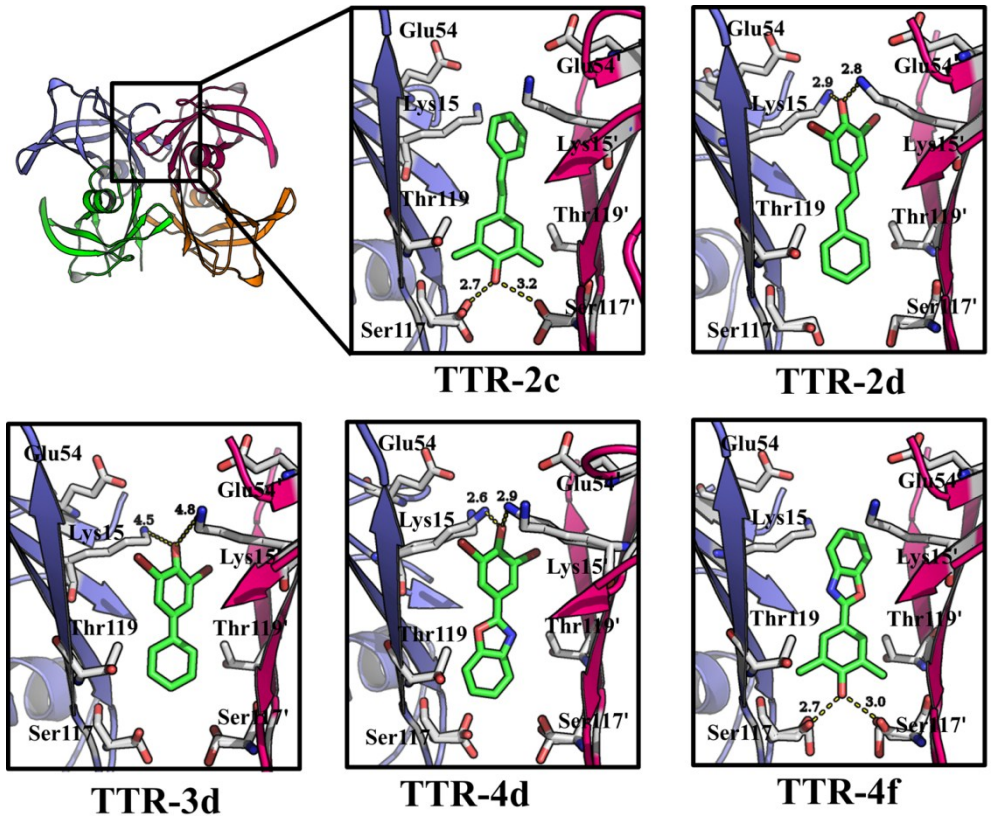

Figure S1 The binding modes of transthyretin amyloidogenesis inhibitors 2c, 2d, 3d, 4d and 4f from their X-ray crystallography structures (PDB id: 3CN0, 3CN1, 3CN2, 2QGD and 2QGC, respectively). The ligands were colored by atom type (carbon atoms in green, bromine in brown and oxygen in red) and were displayed as sticks style. Important interactions including hydrogen bond and electrostatic contact between ligands and key residues were plot as yellow dotted lines.

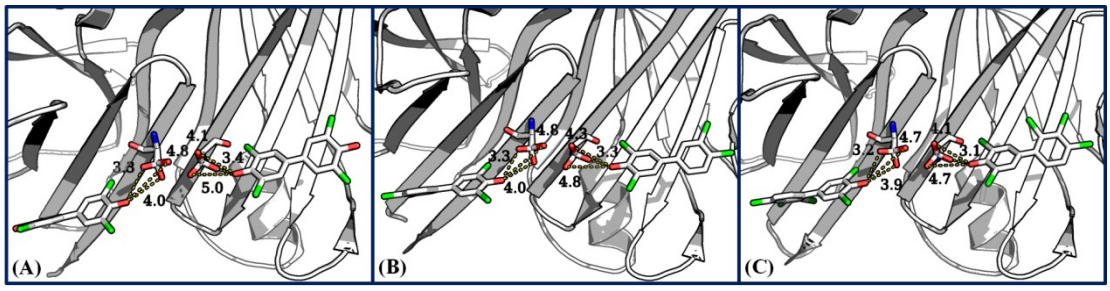

Figure S2 The hydrogen bond distances between multiple conformations of Ser117 and OH-PCBs in the X-ray crystallography structures (PDB id: 2G5U (A), 2GAB (B) and 2G9K (C), respectively).

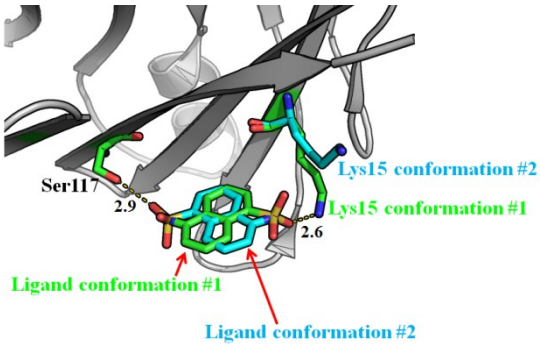

Figure S3 The flexibility of Lys15 induces the multiple bound conformations of ligand at binding pocket of TTR (PDBid: 3CFT)

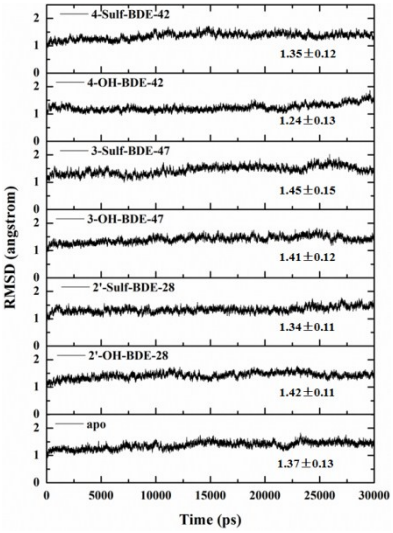

Figure S4 The time evolution of backbone Cα RMSD for apo TTR and 6 TTR-ligand complexes during 30 ns MD simulations.

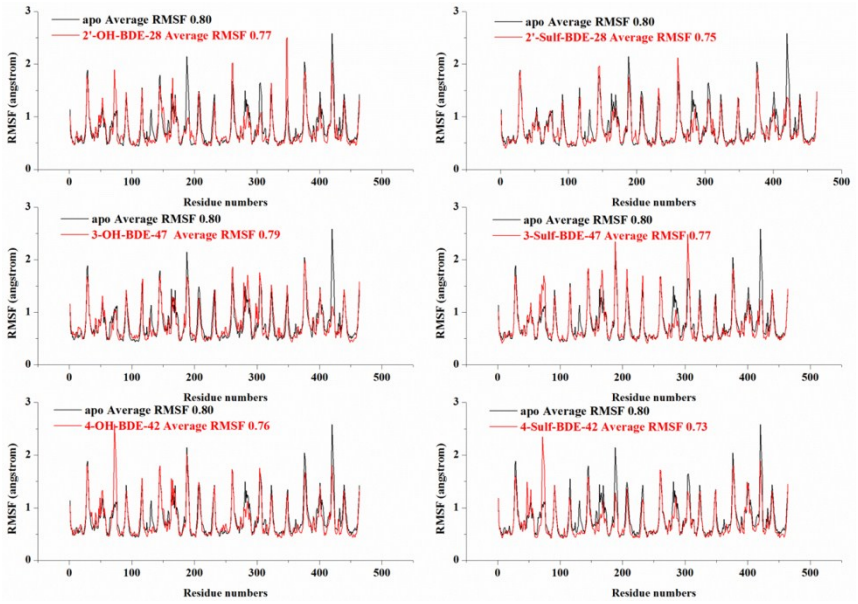

Figure S5 The RMSF of backbone Cα for apo TTR and 6 TTR-ligand complexes during 30 ns MD simulations.

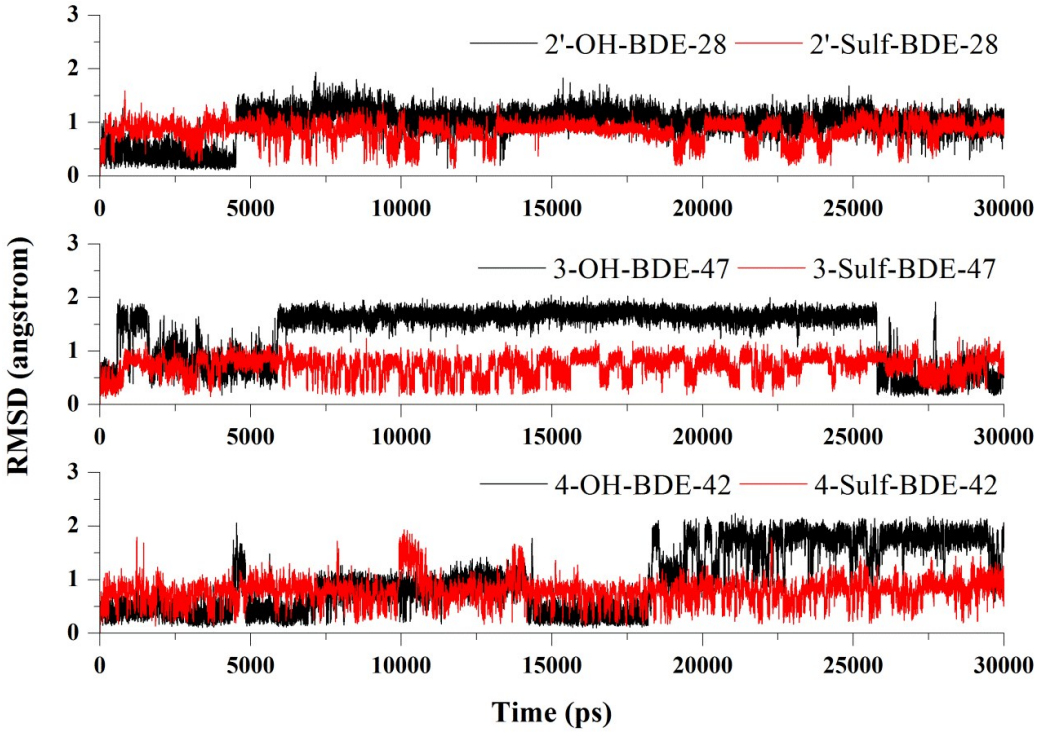

Figure S6 The time evolution of tested ligands RMSD for 6 TTR-ligand complexes during 30 ns MD simulations.

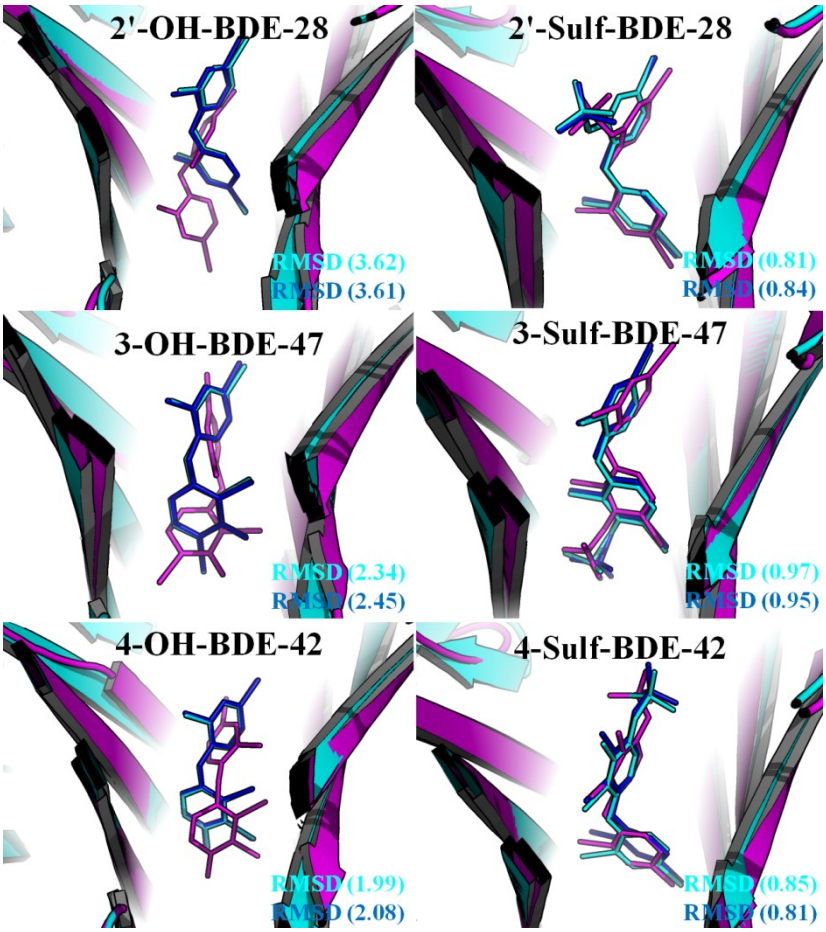

Figure S7 Superimpositions of best-scoring (cyan) and next best-scoring (blue) poses with the representative poses of MD simulations (magenta) based on the clustering results.

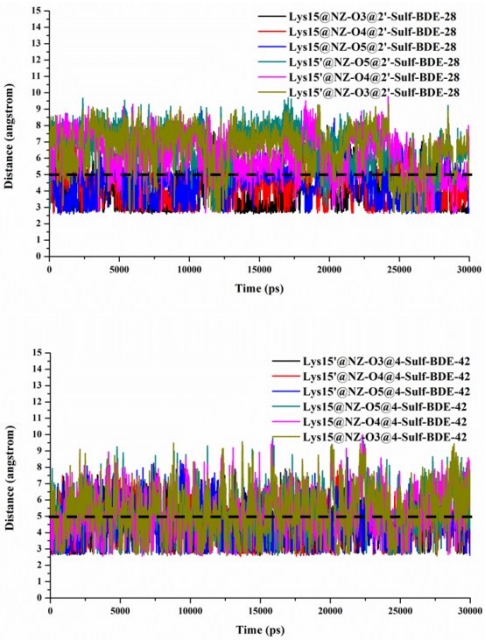

Figure S8 Electrostatic contacts between $–NH_3^+$ groups of Lys15/Lys15' and $–SO_3^-$ groups of ligands in 2'-Sulf-BDE-28 (top) and 4-Sulf-BDE-42 (bottom) complex systems.

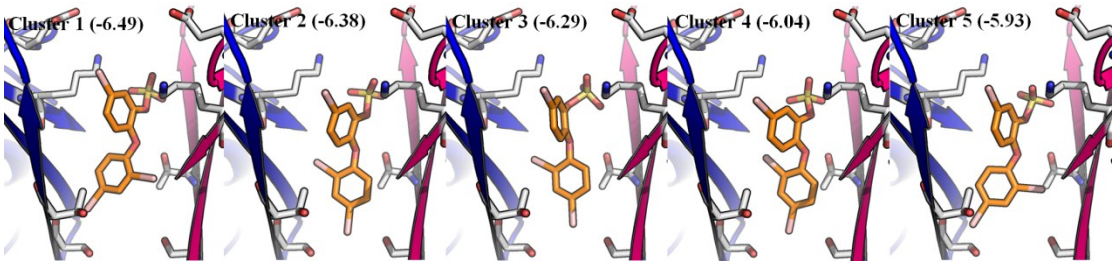

Figure S9 The clustering analysis of LeDock docking results for 2'-Sulf-BDE-28. The first pose of each cluster were displayed and corresponding LeDock scores were showed in parenthesis.

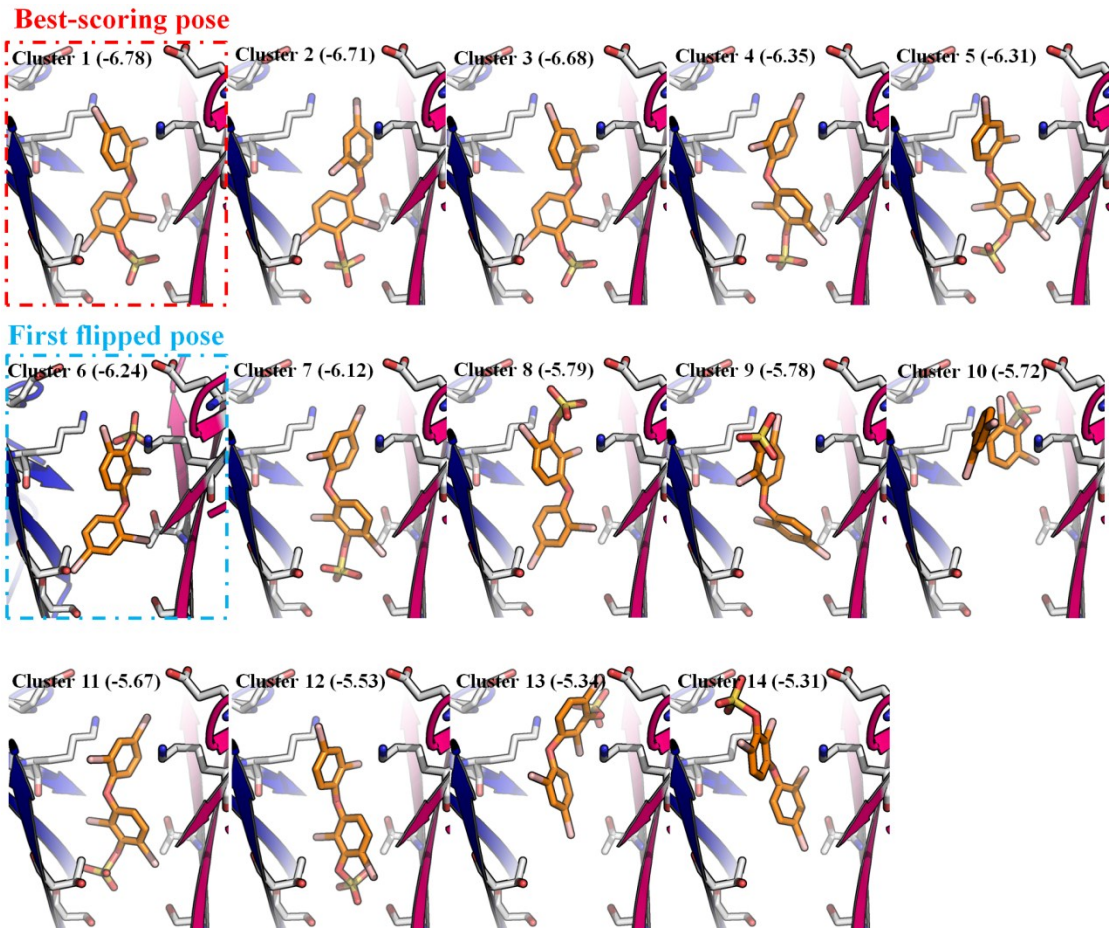

Figure S10 The clustering analysis of LeDock docking results for 3-Sulf-BDE-47. The first pose of each cluster were displayed and corresponding LeDock scores were showed in parenthesis.

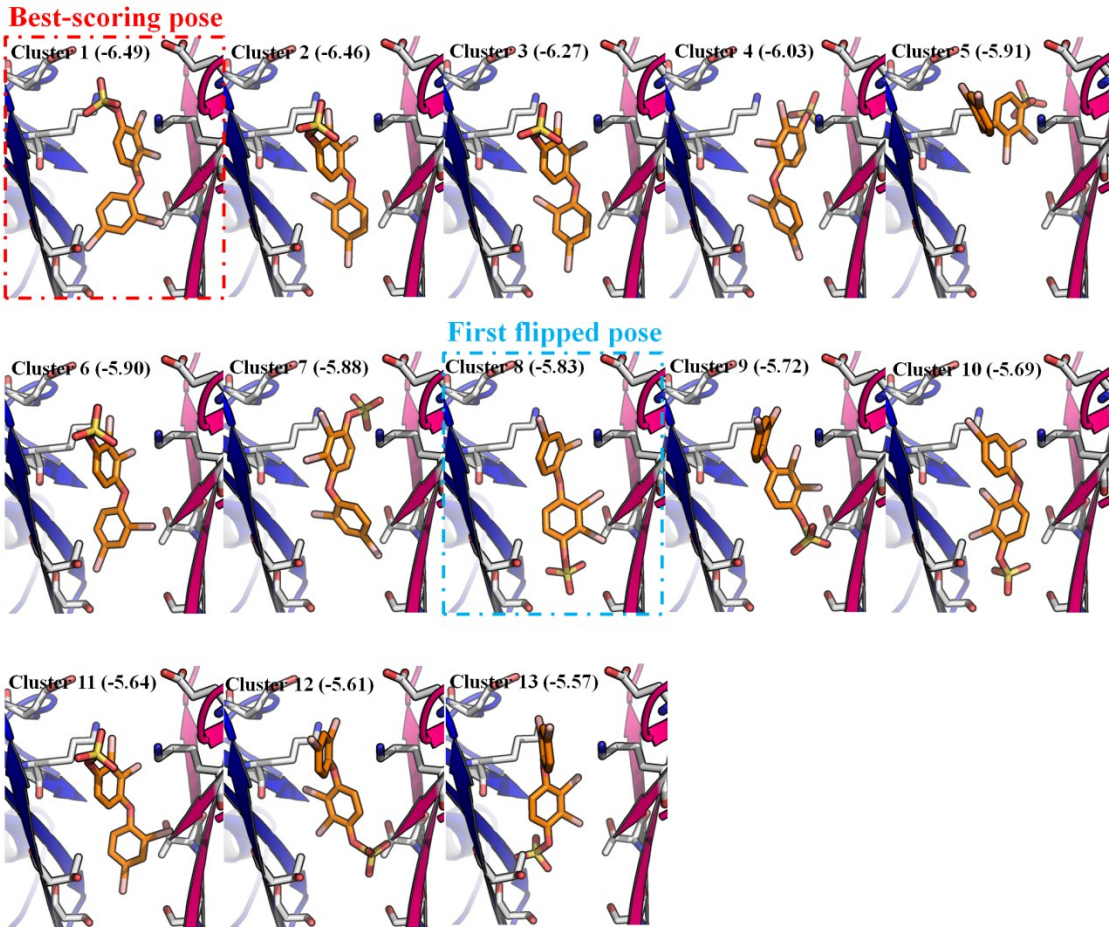

Figure S11 The clustering analysis of LeDock docking results for 4-Sulf-BDE-42. The first pose of each cluster were displayed and corresponding LeDock scores were showed in parenthesis.

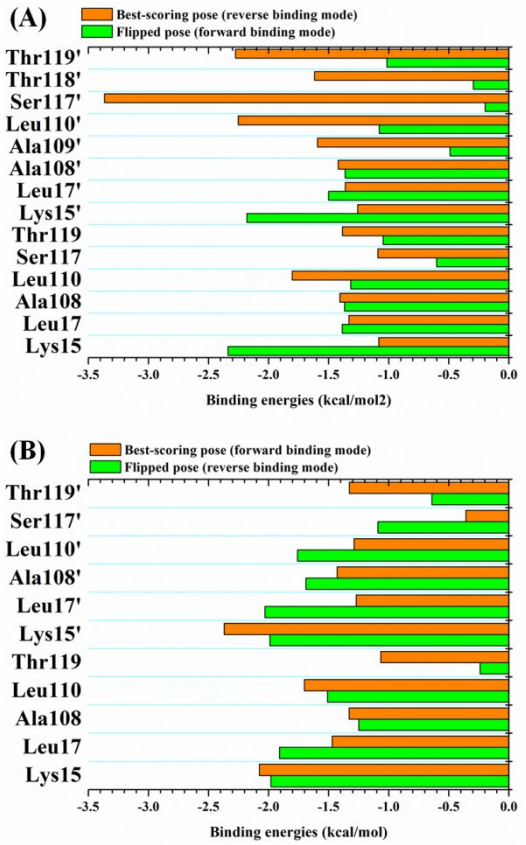

Figure S12 Key residue energy contributions of 3-Sulf-BDE-47 (A) and 4-Sulf-BDE-42 (B) systems for the best-scoring pose and flipped pose.

References

1. G. M. Morris, R. Huey, W. Lindstrom, M. F. Sanner, R. K. Belew, D. S. Goodsell and A. J. Olson, *J. Comput. Chem.*, 2009, **30**, 2785-2791.
2. O. Trott and A. J. Olson, *J. Comput. Chem.*, 2010, **31**, 455-461.
3. H. Li, K. S. Leung, P. J. Ballester and M.-H. Wong, *PLoS One*, 2014, **9**, e85678.
4. H. Li, K. S. Leung, M. H. Wong and P. J. Ballester, *Mol. Inf.*, 2015, **34**, 115-126.
5. K. C. Hsu, Y. F. Chen, S.-R. Lin and J. M. Yang, *BMC Bioinformatics*, 2011, **12**, 1.
6. G. Wu, D. H. Robertson, C. L. Brooks and M. Vieth, *J. Comput. Chem.*, 2003, **24**, 1549-1562.
7. A. N. Jain, *J. Comput. Aided Mol. Des.*, 1996, **10**, 427-440.
8. J. Cao, Y. Lin, L. H. Guo, A. Q. Zhang, Y. Wei and Y. Yang, *Toxicology*, 2010, **277**, 20-28.
9. X. M. Ren and L. H. Guo, *Environ. Sci. Technol.*, 2012, **46**, 4633-4640.
10. T. Hamers, J. H. Kamstra, E. Sonneveld, A. J. Murk, T. J. Visser, M. J. Van Velzen, A. Brouwer and Å. Bergman, *Mol. Nutr. Food Res.*, 2008, **52**, 284-298.
11. T. Hamers, J. H. Kamstra, E. Sonneveld, A. J. Murk, M. H. Kester, P. L. Andersson, J. Legler and A. Brouwer, *Toxicol. Sci.*, 2006, **92**, 157-173.
12. I. A. Meerts, J. J. Van Zanden, E. A. Luijks, I. van Leeuwen-Bol, G. Marsh, E. Jakobsson, Å. Bergman and A. Brouwer, *Toxicol. Sci.*, 2000, **56**, 95-104.
13. M. Montaño, E. Cocco, C. Guignard, G. Marsh, L. Hoffmann, Å. Bergman, A. C. Gutleb and A. Murk, *Toxicol. Sci.*, 2012, kfs228.
14. W. Xu, A. J. Lucke and D. P. Fairlie, *J. Mol. Graphics Modell.*, 2015, 57, 76-88.